Organic & Biomolecular Chemistry

Cite this: *Org. Biomol. Chem.*, 2011, **9**, 1523

www.rsc.org/obc

PAPER

New dendritic gelator bearing carbazole in each branching unit: selected response to fluoride ion in gel phase†

Defang Xu, Xingliang Liu, Ran Lu,* Pengchong Xue, Xiaofei Zhang, Huipeng Zhou and Junhui Jia

Received 26th September 2010, Accepted 15th November 2010
DOI: 10.1039/c0ob00786b

A new dendritic gelator with carbazole as the building block (**HBCD**) was synthesized. It was found that H-bonding between the amide groups and π–π interaction between the aromatic rings played predominant roles in the gel formation. Meanwhile, significant aggregation-induced emission enhancement was observed in the gel state due to the formation of *J*-aggregates and the restricted molecular motion. Notably, the gel state of **HBCD** can be destroyed upon addition of F^-, accompanied by fluorescence enhancement on account of the formation of N–H $\cdots$ F^-, which could further lead to the increased coplanarity of **HBCD**. The sensory capability of **HBCD** exhibited a high selectivity towards F^- instead of the Cl^-, Br^-, I^- and AcO^- anions, which could be explained by the fact that the steric hindrance of the dendrimer would go against the interactions between the larger anions and **HBCD**.

Introduction

As a kind of typical soft materials, gels have been of particular interest in colloid chemistry and material science for many years due to their intriguing properties intermediate between a solid and a liquid.[1,2] Although almost all gels currently in widespread use employ polymers as the 'solid-like' phase, recent advances in the gelation of low molecular-weight organic compounds in organic or aqueous liquids provide a unique methodology to create novel soft matters, which can be extremely responsive to external stimuli due to the gelators being held together by reversible non-covalent interactions. Moreover, great effort has been devoted to developing new chemical structures that can be used to underpin the formation of supramolecular gels on account of their applications in the fields of tissue engineering, biomineralization, and molecular electronics.[3] However, as the bridge between low molecular-weight organic and polymeric gelators, dendritic gelators are not extensively studied since these gelators are relatively difficult to synthesize and purify. It is known that dendrimers are nanoscopic hyperbranched macromolecules with well-defined three-dimensional architectures, which are constructed from an interior core with a regular array of branching units.[4] In particular, the 'dendritic function' can be easily achieved from individual dendritic macromolecules driven by multiple non-covalent interactions,[5] and the steric bulk of the dendritic units may favor the directionality in the gelation process.[6] To date, a great number of functional dendrimers with large numbers of repeating π-conjugated moieties have been synthesized, but the reported functional dendritic gelators so far are focused on the flexible dendrimers or dendrons bearing conjugated units at the focal point or at the terminal points.[7–9] We have previously reported the first rigid dendron-based gelator of the second generation of oligocarbazoles, in which only three carbazole units were involved.[10] Therefore, it is still a great challenge to design the incorporation of π-conjugated monomers in each branching unit using dendritic gelators. Herein, a new dendritic gelator **HBCD** with carbazole as the building block (Chart 1) has been synthesized, and amide groups are selected as the linker to connect aromatic rings because they not only provide H-bonding sites that

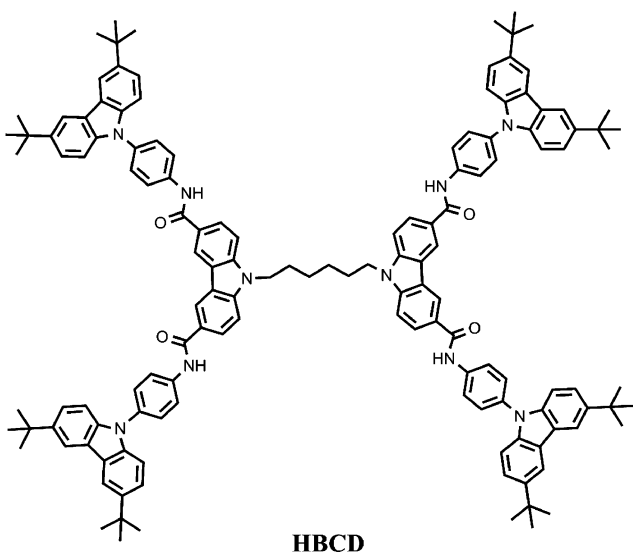

HBCD

Chart 1 Molecular structure of **HBCD**.

State Key Laboratory of Supramolecular Structure and Materials, College of Chemistry, Jilin University, Changchun, 130012, P. R. China. E-mail: luran@mail.jlu.edu.cn; Fax: +86 431 88499179; Tel: +86 431 88499179

† Electronic supplementary information (ESI) available: ^{1}H NMR and MALDI-TOF MS spectra of new compounds; FT-IR spectra of the gel upon addition of anions; SEM image of the destroyed gel; concentration-dependent ^{1}H NMR spectra. See DOI: 10.1039/c0ob00786b

support the molecular assembly, but also act as anion receptors. It is found that **HBCD** could gel DMSO and DMSO-containing mixed solvents efficiently. Notably, the gel state of **HBCD** can be destroyed upon addition of F^-, accompanied by fluorescence enhancement, while no similar behaviors can be detected by addition of other anions, such as Cl^-, Br^-, I^-, AcO^-. Thus, the gel **HBCD** can recognize F^- with selectivity. Herein, we provide a strategy to generate novel gel-phase materials based on dendritic macromolecules with a huge number of functional groups, which favors the expression of the inherent superiority of dendrimers, for example, high sensitivity may be realized from a dendrimer-based fluorescence probe due to more recognition sites, at the supramolecular level.

Results and discussion

Synthesis of HBCD

The synthetic routes for **HBCD** was shown in Scheme 1. Compound **1** was synthesized *via* Ullmann condensation reaction between 3,6-di-tertbutyl-9*H*-carbazole[11] and 1-iodo-4-nitrobenzene in a yield of 90%, and it could be reduced into compound **2** by hydrazine hydrate catalyzed by Pd/C. Meanwhile, the Friedel–Crafts reactions of N-alkyl carbazole derivative **3**, which was prepared *via* alkylation of carbazole with 1,6-dibromohexane in DMF using NaH as a base in a yield of 60%, afforded compound **4**. Then, the hydrolysis of compound **4** in a mixture of KOH, DMSO, ethanol, and H_2O could yield compound **5** with a good yield of 95%. Finally, the target molecule **HBCD** was synthesized in a yield of 60% by the acylation reaction of compound **2** with the corresponding carbonyl chloride, which was obtained from the chlorination of compound **5** with $SOCl_2$ under reflux. The new compounds were characterized by ^1H NMR, FT-IR, MALDI-TOF MS and elemental analyses.

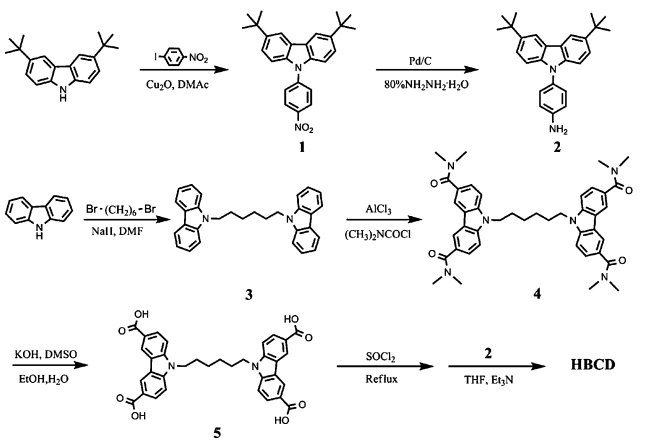

Scheme 1 Synthetic routes for dendritic oligocarbazole **HBCD**.

Gelation behavior of compound HBCD

The gelation property of the carbazole-based dendrimer HBCD was tested in various solvents by means of the "stable to inversion of a test tube" method. From Table 1, we can find that **HBCD** was readily dissolved in THF and DMF but insoluble in aliphatic hydrocarbon solvents, lower alcohols and aromatic solvents, such as n-hexane, cyclohexane, ether petroleum, chloroform, methanol and toluene at room temperature. However, it could gelatinize DMSO and the mixed solvents of DMSO/n-hexane ($v/v = 1/50$), DMSO/toluene ($v/v = 1/5$), DMSO/chloroform ($v/v = 1/10$) and DMSO/ethyl acetate ($v/v = 1/10$). The gel-sol transition temperature (T_{gel}) of HBCD in DMSO was 70 °C at the concentration of 8.3×10^{-3} M, and the critical gelation concentration (CGC) of HBCD was 6.2×10^{-4} M in DMSO, meaning that this dendritic gelator can be classified as a supergelator.[12]

Table 1 Gelation properties of **HBCD** in organic solvents[a]

Solvent	**HBCD**
Hexane	**I**
Cyclohexane	**I**
Petroleum ether	**I**
Toluene	**I**
THF	**S**
Chloroform	**I**
Acetone	**I**
Ethyl acetate	**I**
Methanol	**I**
DMF	**S**
DMSO	**G**
DMSO/hexane ($v/v = 1/50$)	**G**
DMSO/toluene ($v/v = 1/5$)	**G**
DMSO/chloroform ($v/v = 1/10$)	**G**
DMSO/ethyl acetate ($v/v = 1/10$)	**G**
DMSO/methanol	**P**

[a] **G**: gel, **S**: soluble, **I**: insoluble, **P**: precipitate. The low critical gelation concentration (CGC) of **HBCD** is 6.2×10^{-4} M in DMSO.

Self-assembly of HBCD in gel phase

The morphology of DMSO xerogel of carbazole-based dendrimer **HBCD** was investigated by scanning electron microscopy (SEM) and atomic force microscopy (AFM) as shown in Fig. 1. The SEM image revealed a three-dimensional network composed of

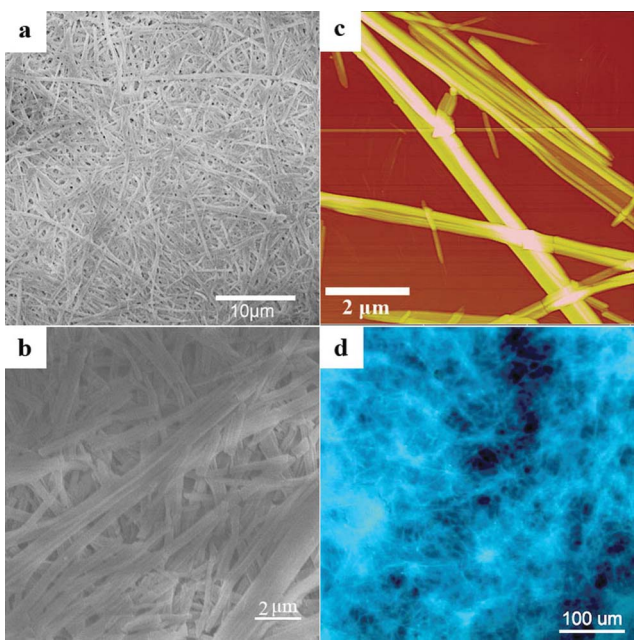

Fig. 1 SEM (a, b), AFM (c) and fluorescence microscopy images (d, λ_{ex} = 330–385 nm) of xerogel **HBCD** obtained from DMSO.

fibrous aggregates with widths of 40–60 nm and length of several μm. In addition, the AFM image of DMSO xerogel based on **HBCD** also showed a bundle of long fibres consisting of thin fibrils. These results suggested that the dendritic macromolecule **HBCD** preferred to self-assemble into one-dimensional nanostructures.

In order to investigate the driving forces leading to the gel formation, FT-IR and ^{1}H NMR spectra of **HBCD** were performed. As shown in Fig. S1,† the amide I band appeared at 1654 cm^{-1} in the gel state, suggesting the formation of intermolecular H-bonding between the amide groups in the fibrous self-assemblies,[13] which could be further confirmed by the temperature-dependent and concentration-dependent ^{1}H NMR spectral changes of **HBCD**. As shown in Fig. 2, we can find a small peak at 10.53 ppm for the NMR signal of the protons in amides in the gel state at 25 °C. As the temperature increased, the peak became stronger and shifted upfield gradually. For instance, it shifted to 10.43 ppm at 45 °C, and to 10.23 ppm at 85 °C. This suggests that the H-bonding could be weakened and even broken at high temperature. Meanwhile, the resonance signals for the protons in amides appeared at $\delta = 10.54$ ppm at high concentration, and shifted upfield to 10.53 ppm at low concentration (Fig. S2†), illustrating that H-bonding played a key role in the aggregation of the dendrimer **HBCD**. Moreover, the peaks corresponding to the aromatic protons appeared in the range of 7.3–8.3 ppm and they were shifted upfield slightly and became stronger with increasing temperature (Fig. 2) or decreasing concentration (Fig. S2†), indicating the π–π interaction between adjacent aromatic moieties in the self-assemblies of **HBCD**,[14] which could be proved further from the evidence of the red shift of the absorption in the gel state compared with that in solution.

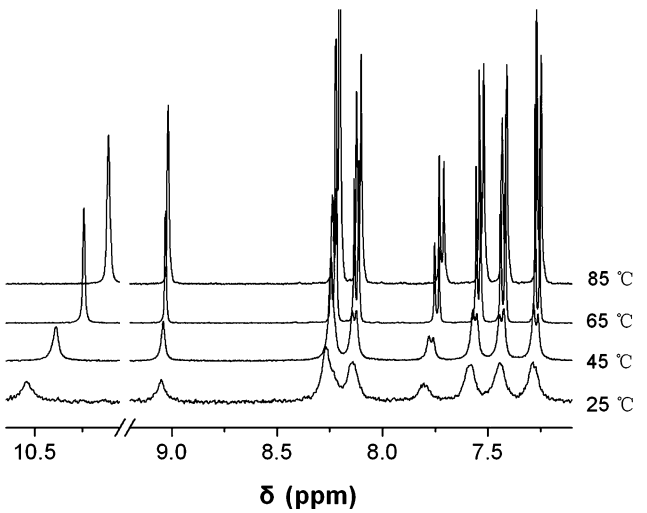

Fig. 2 Temperature-dependent ^{1}H NMR spectra of DMSO-d_6 organogel of **HBCD** (8.3×10^{-4} M).

Photophysical properties

The temperature-dependent UV-vis absorption spectra of **HBCD** in DMSO were recorded to monitor the interaction between the chromophores during the gel formation (Fig. 3). In the hot solution, we found several absorption bands below 360 nm and the maximum appeared at 299 nm, which could be ascribed to π–π* transition. When the temperature was decreased, the absorption intensities were weakened gradually, accompanied by a slight red shift. The maximal absorption peak red shifted to 303 nm in the gel phase, indicating that *J*-aggregates from dendrimer **HBCD** were formed in the gel state.[15] Therefore, we suggested that π–π interactions had an effect on the gel formation.

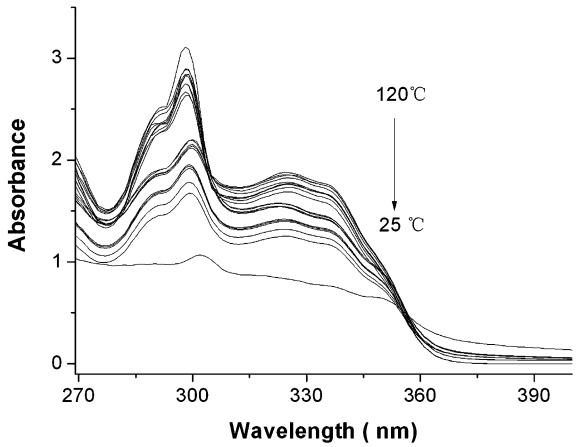

Fig. 3 Temperature-dependent UV-vis spectra of **HBCD** during cooling of the hot solution in DMSO (2.9×10^{-4} M) from 120 °C to 25 °C.

Since the fluorescence spectra can provide important information on the molecular organization of fluorophores, the concentration-dependent fluorescence emission spectra of **HBCD** in DMSO excited at 299 nm were showed in Fig. 4. Only one emission peak at 358 nm was found in dilute solution (1.0×10^{-7} M). When increasing the concentration, a new emission band at *ca.* 460 nm emerged and became stronger and stronger. When the concentration reached 1.0×10^{-5} M, the emission intensity at *ca.* 358 nm was lower than that at *ca.* 460 nm. As a result, we deduced that the emission located at 358 nm originated from the monomeric species, and the one at *ca.* 460 nm could be attributed to the aggregated species. Significantly, a remarkable fluorescence enhancement in the self-assemblies of **HBCD** were found from the temperature-dependent fluorescence spectra as shown in Fig. 5. When excited at 299 nm the fluorescence emission intensity for **HBCD** in the gel phase was almost 40 times stronger than that in hot DMSO solution. In order to confirm the origin of the fluorescence enhancement in DMSO gel, a very weak emission could be observed in the fluorescence spectrum of **HBCD** in

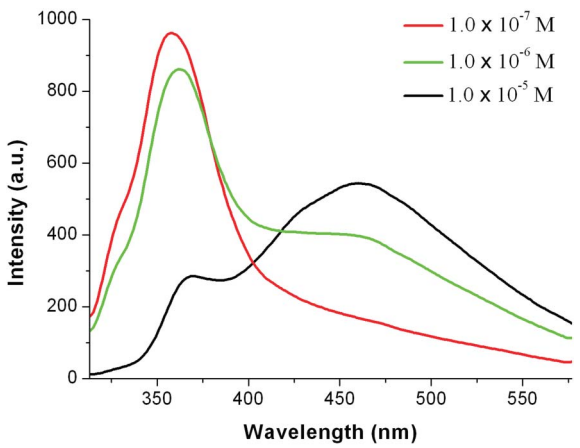

Fig. 4 Fluorescence emission spectra of **HBCD** in DMSO at different concentrations ($\lambda_{ex} = 299$ nm) at 25 °C.

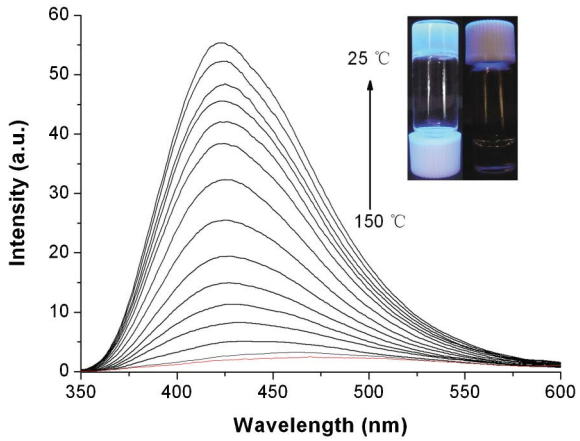

Fig. 5 Temperature-dependent fluorescence emission spectra of **HBCD** in DMSO (black) (8.3×10^{-4} M, λ_{ex} = 299 nm) and in THF (red, 8.3×10^{-4} M, 25 °C). Inset: photograph of the DMSO gel and sol irradiated by 365 nm light.

THF at room temperature, also given in Fig. 5. It meant that the fluorescence enhancement in the self-assemblies of **HBCD** in DMSO originated from the molecular aggregation instead of temperature, which could further confirm the formation of *J*-aggregates in **HBCD**-based gel.[15] Meanwhile, the emission band blue-shifted from 460 nm in the hot solution to 425 nm in the gel state, which was in accordance with the result of the formation of π-aggregates in the gel state. Accordingly, it was clear from Fig. 1d and the inset in Fig. 5 that the gel could emit strong blue light under UV irradiation. In this case, the aggregation-induced emission enhancement of **HBCD**-based gel could be attributed to the synergetic effect of the restricted molecular motion and the formation of *J*-aggregates in the gel state.[16,17]

Anion responsive properties

The effect of anions on the gelation capability was studied by the repeating gelation processes of **HBCD** in DMSO in the presence of anions, including F^-, Cl^-, Br^-, I^- and AcO^-, using their tetrabutylammonium salts as the sources. After 4 equiv tetrabutylammonium fluoride (TBAF, 4 equiv is selected herein because the 4 : 1 complex can be formed from F^- and **HBCD**, which will be discussed below) was added into the DMSO gel of **HBCD** and heated to a clear solution, the precipitation, instead of the gel, could be generated when it was cooled to room temperature. However, the gel state of **HBCD** could be preserved upon the addition of the same amount of other anions (Cl^-, Br^-, I^- and AcO^-). This result indicated that the gel of **HBCD** exhibited a high selectivity towards F^- with naked-eye sensing (Fig. 6).

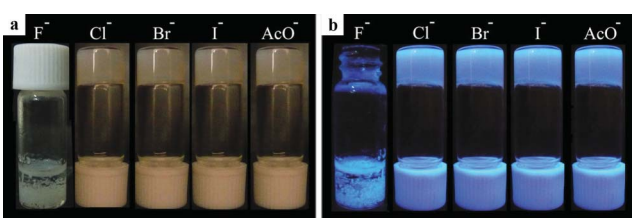

Fig. 6 Photographs of DMSO gels of **HBCD** under daylight (a) and 365 nm light (b) upon addition of 4 equiv of anions.

Since understanding of the interaction between the dendrimer **HBCD** and F^- is of importance in revealing the sensory mechanism, the ^{1}H NMR spectra of **HBCD** upon addition of different amounts of F^- in DMSO-d_6 were investigated. As shown in Fig. 7, the addition of 1–2 equiv of F^- resulted in the weakness and broadening of the peak at δ = 10.5 ppm ascribed to the protons in amides, which indicated the formation of N–H···F^- H-bonds. When 4 equiv of F^- was added, this resonance signal disappeared, which was the same as that upon addition of 10 equiv of F^-. It illustrated that the four amide groups in each dendritic molecule of **HBCD** could be saturated by four fluoride anions *via* H-bonding,[18] and the 1 : 4 complex of **HBCD** and F^- could be formed.[19] FT-IR measurements also confirmed that F^- interacted with **HBCD** *via* H-bonding. As shown in Fig. S1,† the amide I band (1654 cm^{-1}) that emerged in the pure DMSO gel of **HBCD** disappeared when 4 equiv F^- was added, while it was preserved by adding the anions of Cl^-, Br^-, I^- and AcO^-. As a result, H-bonding between amides in the DMSO gel of **HBCD** could be destroyed by addition of F^-, leading to the disappearance of the gel state, in which the 3D network was broken (Fig. S3†).

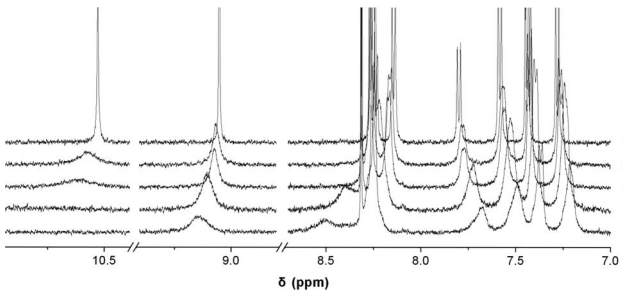

Fig. 7 ^{1}H NMR spectra of **HBCD** (8.0×10^{-4} M) in DMSO-d_6 upon addition different equiv of F^-: (a) 0, (b) 1, (c) 2, (d) 4, and (e) 10.

It should be noted that the emission of **HBCD** could be enhanced during the titration with TBAF, and the emission enhancement was saturated when 4 equiv of F^- was added (Fig. 8a), which further illustrated the formation of the 1 : 4 complex of **HBCD** and F^-. However, no significant fluorescence spectral change was observed upon addition of the anions of Cl^-, Br^-, I^- and AcO^- in gel **HBCD** (Fig. 8b). We deduced that the emission enhancement of **HBCD** upon addition of F^- might be due to the increased coplanarity resulting from the formation of N–H···F^-.[20a,b] The tight binding of the fluoride anion with **HBCD** assisted by H-bonding might increase the activation barrier between twisted conformations, thereby increasing the stability of the photoexcited state. In contrast, it would be difficult

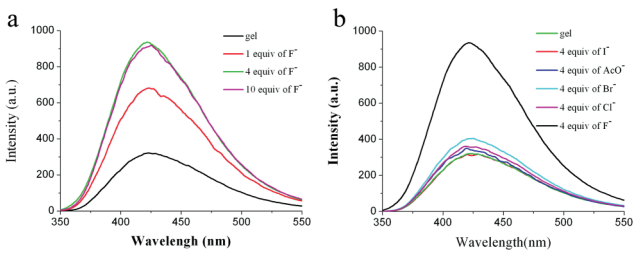

Fig. 8 Fluorescence spectra of the DMSO gel of **HBCD** (1.3×10^{-3} M) upon addition of different equiv of F^- (a) and addition of 4 equiv of anions of F^-, Cl^-, Br^-, I^- and AcO^- (b).

for the larger anions of chloride, bromide, iodide and acetic acid to interact with amide groups in **HBCD** on account of steric hindrance of branched arms.[20c] Therefore, the fluorescence response of **HBCD** exhibited a high selectivity towards F^-.

Conclusion

In summary, we have synthesized a new dendritic gelator using carbazole as the building block, which could form a supergel in DMSO and some DMSO-containing mixed solvents. SEM and AFM images revealed that the dendritic gelator could self-assemble into a 3D network comprising lots of nanofibers with diameters of *ca.* 40–60 nm. Combining the results of FT-IR, ^{1}H NMR, UV-vis and fluorescence emission spectra, we deemed that H-bonding and π–π interactions played key roles in the gel formation. Interestingly, significant aggregation-induced emission enhancement was observed, which could be ascribed to the formation of *J*-aggregates and the restricted molecular motion in the gel state. Notably, we found that the organogel of **HBCD** could allow recognition of F^- selectively since the gel could be destroyed in the presence of F^-, accompanied by the emission enhancement. It can be explained that F^- could interact with **HBCD** *via* H-bonding, leading to the increase of the molecular coplanarity. The reason for the selective sensory capability of **HBCD** towards F^- instead of other anions, such as Cl^-, Br^-, I^-, and AcO^- might be that it was difficult for the larger anions to interact with amide groups in **HBCD** on account of steric hindrance of the branched arms. It provides a strategy to design novel dendritic gelators containing a great deal of functional units, which prefer to self-assemble into 1D organic nanomaterials with desired functionality.

Experimental Section

1. General information

^{1}H NMR spectra were recorded on Mercury plus 500 MHz using $CDCl_3$ and DMSO-d_6 as solvents. Mass spectra were performed on an Agilent 1100 MS series and AXIMA CFR MALDI/TOF (matrix assisted laser desorption ionization/time-of-flight) MS (COMPACT). UV-vis absorption spectra were determined on a Shimadzu UV-1601PC spectrophotometer. Fluorescence spectra were obtained on a Shimadzu RF-5301 luminescence spectrometer. FT-IR spectra were measured using a Nicolet-360 FT-IR spectrometer by incorporating samples in KBr pellet. Scanning electron microscopy (SEM) observations were carried out on a Japan Hitachi model X-650 San electron microscope. The samples for these measurements were prepared by casting the organogel on silicon wafers and drying at room temperature, followed by coating with gold. The atomic force microscopy (AFM) images were obtained on a Nanoscope IIIa AFM Multimode (Digital Instruments, Santa Barbara, CA) under ambient conditions. AFM was operated in the tapping mode with an optical read out using Si cantilevers. C, H, and N elemental analyses were taken with a Perkin–Elmer 240 C elemental analyzer. Fluorescence microscopy images were taken with a fluorescence microscope (Olympus Reflected Fluorescence System BX51, Olympus, Japan).

The preparation of the gel was described as below: the weighted **HBCD** in organic solvent was heated in a sealed test tube in an oil bath until it was dissolved completely. After the solution was allowed to stand at room temperature (25 °C) for several minutes, the state of the mixture was evaluated by the "stable to inversion of a test tube" method.

2. Synthetic procedures and characterizations

3,6-Di-*tert*-butyl-9-(4-nitrophenyl)-9*H*-carbazole (1). 3,6-Di-tertbutyl-9*H*-carbazole (10.0 g, 35.8 mmol), 1-iodo-4-nitrobenzene (8.5 g, 34.1 mmol), Cu_2O (8.0 g, 56 mmol) and DMAc (20 mL) were put sequentially in a seal-tube under nitrogen atmosphere, and the mixture was heated to 180 °C in an oil bath for 20 h. After cooling to room temperature, the mixture was filtrated, and the filtrate was poured into 200 mL H_2O and stirred for several minutes. The solid was collected by filtration and purified by recrystallization from ethanol–THF to give a yellow solid (13.0 g), yield 90%. mp: >250.0 °C. IR (KBr, ν_{max}/cm^{-1}): 3350, 3186, 1649, 1489, 1252. ^{1}H NMR (500 MHz, $CDCl_3$, TMS) δ ppm 8.46 (d, J = 9.0 Hz, 2H), 8.14 (s, 2H), 7.86 (d, J = 9.0 Hz, 2H), 7.51–7.44 (m, 4 H), 1.46 (s, 18 H) (Fig. S4†). Elemental analysis for $C_{26}H_{28}N_2O_2$ calcd: (%) C, 77.97; H, 7.05; N, 6.99; O, 7.99, Found: (%) C, 77.89; H, 6.98; N, 7.06. MALDI-TOF MS: m/z: calcd: 400.2, found: 400.0 (Fig. S5†).

4-(3,6-Di-*tert*-butyl-9*H*-carbazol-9-yl)benzenamine (2). Pd/C (0.4 g) was added into the solution of ethanol (100 mL) containing 3,6-di-*tert*-butyl-9-(4-nitrophenyl)-9*H*-carbazole **1** (9.6 g, 25 mmol), which was heated and refluxed. Then, $NH_2NH_2{\cdot}H_2O$ (80%, 10 mL) was added dropwise to the above hot solution. After refluxing for 10 h, the precipitate was removed by filtration. The filtrate was concentrated and cooled to room temperature. The precipitate was collected and recrystallized from ethanol twice to afford a buff solid (7.5 g), yield 85%. mp: 230.0–232.0 °C. IR (KBr, ν_{max}/cm^{-1}): 3431, 2958, 1620, 1518, 1472. ^{1}H NMR (500 MHz, $CDCl_3$, TMS) δ ppm 8.12 (s, 2 H), 7.44 (d, J = 8.5 Hz, 2H), 7.29 (d, J = 8.5 Hz, 2H), 7.25 (t, J = 1.5 Hz, J = 7.0 Hz, 2H), 6.87 (d, J = 8.5 Hz, 2H), 4.09 (s, 2H), 1.46 (s, 18H) (Fig. S6†). Elemental analysis for $C_{26}H_{30}N_2$ calcd: (%) C, 84.28; H, 8.16; N, 7.56. Found: (%) C, 84.15; H, 8.22; N, 7.67. MALDI-TOF MS: m/z: calcd: 370.2, found: 370.4 (Fig. S7†).

9-(6-(9*H*-carbazol-9-yl)hexyl)-9*H*-carbazole (3). NaH (3.5 g, 6.1 mmol) was added into the solution of DMF (44 mL) containing carbazole (11 g, 65.9 mmol), which was stirred for 15 min at room temperature. Then, 1,6-dibromohexane (4 mL, 26 mmol) was added, and stirred for another 1 h at room temperature. The mixture was poured into 250 mL H_2O, and the solid was collected by filtration. Recrystallization from ethanol–THF (v/v = 20/1) gave a white solid (26 g), yield 95%. mp: 134.0–136.0 °C. IR (KBr, ν_{max}/cm^{-1}): 3049, 2927, 2851, 1593, 1482, 1450, 1325. ^{1}H NMR (500 MHz, DMSO-d_6, TMS) δ ppm 8.08 (d, J = 7.5 Hz, 4H), 7.41 (t, J = 8.0, J = 7.5 Hz, 4H), 7.30 (d, J = 8.0 Hz, 4H), 7.23–7.20 (m, 4H), 4.21 (t, J = 7.5, J = 7.0 Hz, 4H), 1.80 (t, J = 7.0, J = 7.0 Hz, 4H), 1.37–1.34 (m, 4H) (Fig. S8†). Elemental analysis for $C_{30}H_{28}N_2$ calcd: (%) C, 86.50; H, 6.78; N, 6.72. Found: (%) C, 86.35; H, 6.70; N, 6.65. MALDI-TOF MS: m/z: calcd: 416.2, found: 416.3 (Fig. S9†).

9-(6-(3,6-Bis(dimethylcarbamoyl)-9*H*-carbazol-9-yl)hexyl)-N3,N3,N6,N6-tetramethyl-9*H*-carbazole-3,6-dicarboxamide (4). Dimethylearbamic chloride (4.5 mL) in 1,2-dichloroethane

(10 mL) was added into the solution of 9-(6-(9*H*-carbazol-9-yl)hexyl)-9*H*-carbazole **3** (4.0 g, 9.95 mmol) and $AlCl_3$ (6.0 g, 45 mmol) in 1,2-dichloroethane (50 mL) at 0 °C. After refluxing overnight with stirring, the mixture was cooled to room temperature, and poured into H_2O (150 mL). The crude product was extracted with dichloromethane and purified by column chromatography (silica gel, dichloromethane–methanol, v/v = 15/1) to give a blue solid (4.0 g), yield 60%. mp: 164.0–166.0 °C. IR (KBr, ν_{max}/cm^{-1}): 2920, 2843, 1619, 1477, 1382. ^1H NMR (500 MHz, DMSO-d_6, TMS) δ ppm 8.18 (s, 4H), 7.57–7.55 (m, 4H), 7.34 (d, J = 8.5 Hz, 4H), 4.26 (m, 4H), 3.12 (s, 24H), 1.81 (m, 4H), 1.32 (m, 4H) (Fig. S10†). Elemental analysis for $C_{42}H_{48}N_6O_4$ calcd: (%) C, 71.97; H, 6.90; N, 11.99; O, 9.13. Found: (%) C, 71.82; H, 6.78; N, 12.01. MALDI-TOF MS: m/z: calcd: 700.4, found: 701.5 (Fig. S11†).

9-(6-(3,6-Dicarboxy-9*H*-carbazol-9-yl)hexyl)-9*H*-carbazole-3,6-dicarboxylic acid (5). A mixture of compound **4** (4.0 g, 5.7 mmol), KOH (3.2 g, 57.1 mmol), ethanol (50 mL) and DMSO (100 mL) was refluxed with stirring overnight. After cooling to room temperature, the mixture was poured into H_2O (500 mL) and stirred for several minutes. After acidification by dilute hydrochloric acid, the solid was collected by filtration. The solid was washed several times with water and ethanol, and was dried in vacuum at 45 °C. A white solid was obtained (3.2 g), yield 95%. mp: >250.0 °C. IR (KBr, ν_{max}/cm^{-1}): 3433, 2931, 1677, 1599, 1484, 1412, 1294. Elemental analysis for $C_{34}H_{28}N_2O_8$ calcd: (%) C, 68.91; H, 4.76; N, 4.73; O, 21.60. Found: (%) C, 68.84; H, 4.73; N, 4.68. The solubility of **5** was very poor in common organic solvents, so it is difficult to get its ^1H NMR data.

9-(6-(3,6-Bis(4-(3,6-di-*tert*-butyl-9*H*-carbazol-9-yl)phenylcarbamoyl)-9*H*-carbazol-9-yl)phenyl)-N3,N6-bis(4-(3,6-di-*tert*-butyl-9*H*-carbazol-9-yl)phenyl)-9*H*-carbazole-3,6-dicarboxamide (HBCD). Compound **5** (1.0 g, 1.7 mmol) was added to $SOCl_2$ (5 mL) and refluxed for 2 h. After removing the surplus $SOCl_2$ by vacuum distillation, a blue solid was obtained and diluted with dry THF directly. The solution was added dropwise to the dry THF (15 mL) solution of compound **2** (3.07 g, 8.3 mmol) and triethylamine (0.48 mL) at 0 °C. After stirring at room temperature for 12 h, the solution was poured into water (200 mL), and the precipitate was filtered. The crude product was recrystallized from ethanol twice to give a white solid (2.0 g), yield 60%. mp: >250.0 °C. IR (KBr, ν_{max}/cm^{-1}): 3419, 2960, 1648, 1516, 1484. ^1H NMR (500 MHz, DMSO-d_6, TMS) δ ppm 10.37 (s, 4H), 9.03 (s, 4H), 8.24 (d, J = 7.5 Hz, 12H), 8.13 (d, J = 8.5 Hz, 8H), 7.75 (d, J = 8.5 Hz, 4H), 7.55 (d, J = 8.5 Hz, 8H), 7.43 (d, J = 8.5 Hz, 8H), 7.27 (d, J = 8.5 Hz, 8H), 4.49 (t, J = 6.5, J = 6.5 Hz, 4H), 1.84 (t, J = 5.0, J = 2.0 Hz, 4H), 1.40 (s, 76H) (Fig. S12, S13†). Elemental analysis for $C_{30}H_{28}N_2$ calcd: (%) C, 82.76; H, 7.05; N, 6.99; O, 3.20. Found: (%) C, 82.65; H, 6.93; N, 7.08. MALDI-TOF MS: m/z: calcd for 2002.1; found: 2001.1 (Fig. S14†).

Acknowledgements

This work is financially supported by the National Natural Science Foundation of China (20874034 and 51073068), 973 Program (2009CB939701), NSFC-JSPS Scientific Cooperation Program (21011140069) and Open Project of State Key Laboratory of Supramolecular Structure and Materials (SKLSSM200901).

Notes and references

1 (*a*) P. J. Flory, *Principles of Polymer Chemistry*, Cornell University Press, Ithaca, 1953; (*b*) P. J. Flory, *Faraday Discuss. Chem. Soc.*, 1974, **57**, 7–18.
2 K. Kajiwara and Y. Osada, *Gels Handbook*, Vol. 1–4, Academic Press, San Diego, 2000.
3 A. R. Hirst, I. A. Coates, T. R. Boucheteau, J. F. Miravet, B. Escuder, V. I. Castelletto, W. Hamley and D. K. Smith, *J. Am. Chem. Soc.*, 2008, **130**, 9113–9121.
4 (*a*) J. M. J. Fréchet, *Science*, 1994, **263**, 1710–1715; (*b*) D. A. Tomalia, *Adv. Mater.*, 1994, **6**, 529–539; (*c*) M. Fischer and F. Vögtle, *Angew. Chem. Int. Ed.*, 1999, **38**, 885–905; (*d*) D. A. Tomalia and R. Esfand, *Chem. Ind.*, 1997, **11**, 416–420.
5 (*a*) A. R. Hirst and D. K. Smith, *Top. Curr. Chem.*, 2005, **256**, 237–273; (*b*) D. K. Smith, *Chem. Commun.*, 2006, 34–44.
6 D. K. Smith, *Adv. Mater.*, 2006, **18**, 2773–2778.
7 (*a*) W. D. Jang, D. L. Jiang and T. Aida, *J. Am. Chem. Soc.*, 2000, **122**, 3232–3233; (*b*) W. D. Jang and T. Aida, *Macromolecules*, 2003, **36**, 8461–8469.
8 (*a*) J. G. Hardy, A. R. Hirst, D. K. Smith, C. Brennanb and I. Ashworth, *Chem. Commun.*, 2005, 385–387; (*b*) A. R. Hirst and D. K. Smith, *Chem.–Eur. J.*, 2005, **11**, 5496–5508; (*c*) A. R. Hirst, J. F. Miravet, B. Escuder, L. Noirez, V. Castelletto, I. W. Hamley and D. K. Smith, *Chem.–Eur. J.*, 2009, **15**, 372–379.
9 (*a*) Y. Ji, Y. F. Luo, X. R. Jia, E. Q. Chen, Y. Huang, C. Ye, B. B. Wang, Q. F. Zhou and Y. We, *Angew. Chem., Int. Ed.*, 2005, **44**, 6025–6029; (*b*) Y. Ji, G. C. Kuang, X. R. Jia, E. Q. Chen, B. B. Wang and W. S. Li, *Chem. Commun.*, 2007, 4233–4235; (*c*) G. C. Kuang, Y. Ji, X. R. Jia, Y. Li, E. Q. Chen and Y. Wei, *Chem. Mater.*, 2008, **20**, 4173–4175.
10 X. C. Yang, R. Lu, F. Y. Gai, P. C. Xue and Y. Zhan, *Chem. Commun.*, 2010, **46**, 1088–1090.
11 T. H. Xu, R. Lu, X. L. Liu, X. Q. Zheng, X. P. Qiu and Y. Y. Zhao, *Org. Lett.*, 2007, **9**, 797–800.
12 (*a*) R. G. Weiss, and P. Terech, *Molecular Gels: Materials with Self-Assembled Fibrillar Networks*, Springer, Dordrecht, 2006; (*b*) F. Würthner, C. Bauer, V. Stepanenko and S. Yagai, *Adv. Mater.*, 2008, **20**, 1695; (*c*) S. J. George and A. Ajayaghosh, *Chem.–Eur. J.*, 2005, **11**, 3217–3227; (*d*) R. Luboradzki, O. Gronwald, A. Ikeda and S. Shinkai, *Chem. Lett.*, 2000, 1148–1152 .
13 (*a*) X. C. Yang, R. Lu, P. C. Xue, B. Li, D. F. Xu, T. H. Xu and Y. Y. Zhao, *Langmuir*, 2008, **24**, 13730–13735; (*b*) Y. M. Zhang, Q. Lin, T. B. Wei, X. P. Qin and Y. L, *Chem. Commun.*, 2009, 6074–6076; (*c*) X. Y. Yang, G. X. Zhang, D. Q. Zhang and D. B. Zhu, *Langmuir*, 2010, **26**, 11720–11725.
14 P. C. Xue, R. Lu, X. C. Yang, L. Zhao, D. F. Xu, Y. Liu, H. Z. Zhang, H. Nomoto, M. Takafuji and H. Ihara, *Chem.–Eur. J.*, 2009, **15**, 9824–9835.
15 (*a*) P. Chen, R. Lu, P. C. Xue, T. H. Xu, G. J. Chen and Y. Y. Zhao, *Langmuir*, 2009, **25**, 8395; (*b*) X. C. Yang, Ran. Lu, H. P. Zhou, P. C. Xue, F. Y. Wang, P. Chen and Y. Y. Zhao, *J. Colloid Interface Sci.*, 2009, **339**, 527–532; (*c*) K Miyamoto, T Sawada, H Jintoku, M Takashi, T Sagawa and H Ihara, *Tetrahedron Lett.*, 2010, **51**, 4666–4669.
16 Y. L. Chen, Y. X. Lv, Y. Han, B. Zhu, F. Zhang, Z. S. Bo and C. Y. Liu, *Langmuir*, 2009, **25**, 8548–8555.
17 S. Kim, Q. D. Zheng, G. S. He, D. J. Bharali, H. E. Pudavar, A. Baev and P. N. Prasad, *Adv. Funct. Mater.*, 2006, **16**, 2317–2323.
18 (*a*) T. H. Kim, M. S. Choi, B. H. Sohn, S. Y. Park, W. S. Lyood and T. S. Lee, *Chem. Commun.*, 2008, 2364–2366; (*b*) J. E. A. Webb, M. J. Crossley, P. Turner and P. Thordarson, *J. Am. Chem. Soc.*, 2007, **129**, 7155–7162; (*c*) H. Maeda, Y. Haketa and T. Nakanishi, *J. Am. Chem. Soc.*, 2007, **129**, 13661–13674; (*d*) H. Yang, T. Yi, Z. G. Zhou, Y. F. Zhou, J. C. Wu, M. Xu, F. Li and C. H. Huang, *Langmuir*, 2007, **23**, 8224–8230.
19 R. J. Varghese, S. J. George and A. Ajayaghosh, *Chem. Commun.*, 2005, 593–595.
20 (*a*) M. Cametti and K. Rissanen, *Chem. Commun.*, 2009, 2809–2829; (*b*) T. D. Thangadurai, N. J. Singh, In-Chul. Hwang, J. W. Lee, R. P. Chandran and K. S. Kim, *J. Org. Chem.*, 2007, **72**, 5461–5464; (*c*) G. X. Xu and M. A. Tarr, *Chem. Commun.*, 2004, 1050–1051.

